

# Epigenetic silencing of *KCTD8* promotes hepatocellular carcinoma growth by activating PI3K/AKT signaling

Jing Zhou<sup>a,b</sup> , Meiying Zhang<sup>b</sup> , Aiai Gao<sup>b</sup> , James G Herman<sup>c</sup>  and Mingzhou Guo<sup>\*,a,b,d</sup> 

<sup>a</sup>School of Medicine, NanKai University, Tianjin, 300071, China; <sup>b</sup>Department of Gastroenterology & Hepatology, the First Medical Center, Chinese PLA General Hospital, Beijing, 100853, China; <sup>c</sup>The Hillman Cancer Center, University of Pittsburgh Cancer Institute, Pittsburgh, PA 15213, USA; <sup>d</sup>National Key Laboratory of Kidney Diseases, Beijing, 100853, China

## ABSTRACT

**Aim:** The aim of current study is to explore the epigenetic changes and function of *KCTD8* in human hepatocellular carcinoma (HCC).

**Materials & methods:** HCC cell lines and tissue samples were employed. Methylation specific PCR, flow cytometry, immunoprecipitation and xenograft mouse models were used.

**Results:** *KCTD8* was methylated in 44.83% (104/232) of HCC and its methylation may act as an independent poor prognostic marker. *KCTD8* expression was regulated by DNA methylation. *KCTD8* suppressed HCC cell growth both *in vitro* and *in vivo* via inhibiting PI3K/AKT pathway.

**Conclusion:** Methylation of *KCTD8* is an independent poor prognostic marker, and epigenetic silencing of *KCTD8* increases the malignant tendency in HCC.

## ARTICLE HISTORY

Received 21 March 2024  
Accepted 14 June 2024

## KEYWORDS

DNA methylation; hepatocellular carcinoma; *KCTD8*; PI3K/AKT signaling pathway; tumor suppressor

## 1. Background

Hepatocellular carcinoma (HCC) is a highly fatal malignant cancer with 5-year overall survival (OS) of approximately 18% [1,2]. The infection of Hepatitis B and C viruses was considered to be the main cause of HCC. HBV vaccine inoculation and antiviral therapy have decreased the incidence apparently [2]. However, other risk factors, such as nonalcoholic steatohepatitis and alcoholic liver disease, are becoming increasingly important [3]. Molecular alterations in genomics have been extensively studied to develop targeting therapeutics in various cancers. However, the genomic-based precision has not been well established in HCC and most mutations are not actionable [4–6]. Sorafenib was the first approved multi-target tyrosine kinase inhibitor for advanced-stage HCC. Then, lenvatinib was approved for first-line therapy. Regorafenib and cabozantinib were approved for second-line treatment. However, the efficacy of these inhibitors is modest in improving patient outcomes [5,7,8]. Finding new curative therapeutic approaches is urgently needed. Better understanding the mechanism of HCC may develop novel therapeutic strategies. A few signaling pathways have been found playing important roles in HCC initiation and progression, such as Ras/Raf/MAPK, PI3K/Akt/mTOR, JAK/STAT, Wnt/ $\beta$ -catenin, Hippo, Notch

and Hedgehog pathways [5,9]. It is noticeable that certain signaling pathways may exhibit conflicting roles under diverse environments in HCC, such as Wnt/ $\beta$ -catenin and NF- $\kappa$ B signaling pathways [10]. The contradictory effects may be attributed to distinct mechanisms, such as NF- $\kappa$ B signaling, which is involved in both inflammation and DNA damage repair (DDR). Furthermore, in addition to driver gene mutations that activate cancer-related signaling pathways, the epigenetic silencing of tumor suppressor gene expression can also contribute to carcinogenesis by disrupting signaling transduction [11–13]. Dysregulation of these signaling pathways represents a major mechanism of cancer development. Remarkable efficacy was observed in lung cancer with *EGFR* mutation by targeting tyrosine kinase. Most of targeting drugs approved in clinic were mainly specific to proteins encoded by mutated oncogenes. However, therapeutic targeting some of oncogenes was challenged due to lack of enzymatic activity or proper binding sites for drugs, such as transcription factor MYC [14–17]. Gene mutation and epigenetic abnormality of tumor suppressors were usually regarded as undruggable [18–20]. Epigenetic alterations are more frequently in cancer compared with driver gene mutations [21]. Epigenetic regulation plays important roles in growth-related pathways by

**CONTACT** Mingzhou Guo Tel.: +86 10 66937651;  [mzguo@hotmail.com](mailto:mzguo@hotmail.com)

 Supplemental data for this article can be accessed at <https://doi.org/10.1080/17501911.2024.2370590>

© 2024 The Author(s). Published by Informa UK Limited, trading as Taylor & Francis Group  
This is an Open Access article distributed under the terms of the Creative Commons Attribution-NonCommercial-NoDerivatives License (<http://creativecommons.org/licenses/by-nc-nd/4.0/>), which permits non-commercial re-use, distribution, and reproduction in any medium, provided the original work is properly cited, and is not altered, transformed, or built upon in any way. The terms on which this article has been published allow the posting of the Accepted Manuscript in a repository by the author(s) or with their consent.

regulating the expression of its key component. Similar with genetic alterations, epigenomic changes may also cause peculiar phenotypes in cancer. As epigenetic modifications are potentially reversible, therapeutics by targeting epigenetic regulating enzymes are becoming promising anticancer treatment. However, the toxicity of these reagents was constantly reported in pre-clinical and clinical trials [22]. Epigenetic-based “synthetic lethality” innovated the strategy of targeting therapy [23–26]. To exploit more effective therapeutic strategies, it is necessary to clarify the regulatory network of cell fate or DDR-related signaling pathways, as well as the aberrant alterations of their key components in cancer.

The potassium channel tetramerization domain (KCTD) family is composed of 25 members [27]. At the N-terminal, these proteins share a conserved BTB (Broad complex, Tramtrak and Bric-a-brac)/POZ (poxvirus zinc finger) domain, which is a motif (95 amino acids) to perform biological function and protein-protein interaction [28–31]. The C-terminal sequences of KCTD proteins are highly variable [32]. Most studies related to these proteins have focused mainly on the pathophysiology of neurodevelopmental diseases [31,33,34]. The biological functions of most KCTD family members are not well characterized. A few KCTD members have been identified to participate in development and tumorigenesis by involving in different signal transduction pathways [27]. KCTD9 was found to suppress colorectal cancer growth by inhibiting Wnt signaling, while KCTD12 was shown to inhibit AKT signaling in breast cancer [35,36]. Additionally, KCTD5 was observed to inhibit the PI3K/AKT pathway in HEK293T cells and KCTD5 was interacted with KCTD8 through the C-terminal [37,38]. The methylation status of *KCTD8* in breast cancer was detected by utilizing a combined approach involving the methyl-CpG enrichment technique and microarray-based comparative genomic hybridization assay [39]. In this study, the mechanism and expression regulation of *KCTD8* were investigated in HCC.

## 2. Materials & methods

### 2.1. HCC cell lines & primary tumor samples

Bel-7405, PLC/PRF5, HCCLM3, SNU449 and Huh7 cell lines were utilized. All cell lines were cultured in RPMI-1640 medium (Gibco, #31800089) or DMEM (Gibco, #12100061) supplemented with 1% penicillin/streptomycin solution (Biosharp, #BL505A) and 10% fetal bovine serum. STR profiling for authentication and mycoplasma detection were performed in these cells. A total of 232 cases of primary HCC without chemo or radiotherapy before surgery were collected in the Department of Hepatobiliary Surgery of

Chinese PLA General Hospital from 2009 to 2019. Fresh HCC tissue samples were immediately snap-frozen and stored at  $-80^{\circ}\text{C}$  after surgery. All samples obtained were diagnosed as primary HCC by pathological manifestation. TNM stage was performed by the 8th Edition of AJCC. All protocols were approved by the Ethics Committee of the Chinese PLA General Hospital (IRB number: 20090701-015).

### 2.2. RNA preparation, DNA modification & PCR amplification

HCC cells were seeded at a density of  $\sim 30\%$  confluence for growing 12 h. The medium was changed every 24 h during cell treatment with  $2\ \mu\text{M}$  5-aza (Sigma, #A3656) for 96 h. TRIzol (Invitrogen, #15596026) was utilized to extract total RNA. Five micrograms of RNA was utilized for synthesizing cDNA (Thermo Fisher Scientific, #K1691). Each reaction included  $20\ \mu\text{l}$  mixture and was diluted to  $100\ \mu\text{l}$ . To avoid experimental bias, 5 reactions were mixed together after cDNA quality assessment. Primers sequences of KCTD8 for reverse transcription PCR (RT-PCR) are as below: 5'-CATGGTGCGTGAAGTCC T-3' (forward), 5'-GGGAGTGCTTGCCCTCTGAAT-3' (reverse). The GAPDH primer sequences used for internal control and the detailed thermal cycling parameters were as previously described [25].

Genomic DNA extraction and sodium bisulfite modification were performed as previously [25]. Methylation was detected by methylation-specific PCR (MSP). The MSP primer sequences are as below: 5'-CGTTGTTTCGAATTTTG AGCGGGGTC-3' (methylation sense), 5'-TACACTTCTCGT TCCCCGAAACCCG-3' (methylation antisense); 5'-TGTTGTT GTTTTGAATTTTGAGTGGGGTT-3' (unmethylation sense), 5'-ACTACTTTTCTCATTCCCCAAAACCCA-3' (unmethylation antisense). The amplification conditions were described previously [25].

### 2.3. Construction of KCTD8 vectors & identification of KCTD8 expressing monoclonal cells

The human *KCTD8* (GenBank accession number: NM\_386617) coding region was applied for the construction of expression vector with pCDH-CMV-MCS-puro plasmid. Primers for amplification were designed as below: 5'-TGCTCTAGACTATGGCTCTGA AGGACAC-3' (forward), 5' CGGGATCCCTATAACCCATA CTCTGCAAC-3' (reverse). KCTD8 expressing or empty vectors with packaging plasmids (pLP1, pLP2 and VSVG) were transfected into HEK293T cells with Lipofectamine 3000 reagent (Invitrogen, #L3000008) following the manufacturer's instructions. The lentiviral supernatant was collected after culturing the cells for 48 h and then was filtered through a  $0.22\ \mu\text{m}$  filter membrane.

Subsequently, the lentiviral supernatant was added into Bel-7405 and PLC/PRF5 cell culture medium at a ratio of 1:1. The polybrene (Sigma-Aldrich, #H9268) was added into the culture medium at a final concentration of 10  $\mu\text{g/ml}$  to enhance transfection efficiency. The medium was replaced with fresh RPMI-1640 after growing for 12 h. Cells were treated with puromycin (MCE, #HY-15695) for 3 days at a concentration of 1.0  $\mu\text{g/ml}$ . Limited dilution assay was utilized to obtain monoclonal cells for expression of KCTD8, which was further validated by western blot.

#### 2.4. SiRNA knockdown technique

RNAiMax (Invitrogen, #13778075) was utilized to knock down IMPDH2. The targeting siRNA sequences of IMPDH2 were as below: sense-siRNA#1: 5'-GGA CAGACCUGAAGAAGAATT-3'; antisense-siRNA#1: 5'-UUCUUCUUCAGGUCUGUCCTT-3'; sense-siRNA#2: 5'-GCAGCCAGAACAGAUUUUTT-3'; antisense-siRNA#2: 5'-AAAUAUCUGUUCUGGCUGCTT-3'; sense-siRNA#3: 5'-GCCAGGACAUUGGUGCCAATT-3'; antisense-siRNA#3: 5'-UUGGCACCAAUGUCCUGGCTT-3'. The efficiency was validated by western blot.

#### 2.5. MTT, colony formation & transwell assays

Bel-7405 and PLC/PRF5 cells with or without KCTD8 expression were plated into 96-well plates at an initial density of 2000 cells per well. The MTT assay was utilized to evaluate the ability of cell proliferation at the time point of 0, 24, 48, 72 and 96 h (KeyGEN Biotech, # KGT5251). The OD values were detected at a wavelength of 490 nm. For the colony formation assay, KCTD8 silenced and re-expressed Bel-7405 and PLC/PRF5 cells were inoculated into 6-well plates at a density of 500 cells each well. Cells were fixed and stained with crystal violet 12 days after seeding (Solarbio, #C8470).

For the migration study,  $3 \times 10^4$  cells were added to the upper chamber (Corning, #3422) and grown for 24 h. Cells that migrated to the lower surface of the membrane were fixed and stained following previous description and images were taken under a microscope. For the invasion assay, cells ( $3 \times 10^4$ ) were suspended into the upper chamber of the Transwell apparatus coated with Matrigel (Becton-Dickinson Biosciences, #356234), and similar procedures with migration assay were performed. All the experiments were triplicated.

#### 2.6. Western blot & immunoprecipitation assays

Detailed procedure of western blot was described in previous study [25]. Antibodies used were listed as below: KCTD8 (Lifespan, #LS-C165463-400), MMP2 (Proteintech, #10373-2-P), MMP7 (Proteintech, #10374-2-

P), MMP9 (Proteintech, #27306-1-AP), caspase-3/cleaved caspase-3 (Proteintech, #19677-1-AP), BAX (Cell Signaling Technology, #2772S), BCL-2 (Cell Signaling Technology, #4223S), IMPDH2 (Proteintech, #67663-1-Ig), AKT (Abcam, #ab8805), Ser473-p-AKT (Cell Signaling Technology, #4060S), PI3K110 $\beta$  (Proteintech, #67121-1-Ig),  $\beta$ -actin (Beyotime, #AF0003), mTOR (Cell Signaling Technology, #2972S) and Ser2448-p-mTOR (ZENBIO, #R381548). IP technique is briefly described as below. Cell lysates were incubated with an antibody overnight and then incubated with protein A/G agarose beads (YEASEN, #36403ES08) for 4 h at 4°C. The beads were collected and washed to obtain the co-precipitated proteins. Products were separated and examined by SDS-PAGE and stained with silver. The bands that were clearly distinguishable in the experimental group but not in the IgG group were excised for further mass spectrometry analysis.

#### 2.7. Apoptosis analysis

FACScan Flow Cytometer was utilized for apoptosis analysis. Cells were stained with the Annexin V-FITC/PI Apoptosis Detection Kit and followed the manufacturer's instructions (KeyGen Biotech, #KGA106). The experiments were triplicated.

#### 2.8. HCC cell xenograft tumor model

Nude mice were ordered from SBF Biotech (Beijing, China) and grouped randomly ( $n = 6$ ). Bel-7405 cells ( $3 \times 10^6$ ) without or with KCTD8 expression were inoculated into mice subcutaneously. The inoculation position was in right side of dorsal. The volume was calculated using the formula:  $V = L \times W^2/2$ . Tumor volume was examined every 3 days. The levels of KCTD8 (Lifespan, #LS-C165463-400), PI3K110 $\beta$  (Proteintech, #67121-1-Ig), p-AKT (Cell Signaling Technology, #4060S), p-mTOR (ZENBIO, #R381548) and ki67 (ZSBIO, TA800648) in xenografts were assessed by IHC. They were diluted to 1:50, 1:400, 1:500, 1:200 and 1:500, respectively. H score was used to quantify the degree of immunostaining according to the staining intensity and the percentage of positive cells. All the animal experiment protocols were performed according to the Animal Ethics Committee at Chinese PLA General Hospital (approval number: 2022-X18-72).

#### 2.9. Statistical analysis

SPSS 21.0 software and GraphPad Prism 8.0 were utilized for statistical analysis. The chi-square test was performed for independent dichotomous variables. For difference comparison in two experimental groups, the student's t test was employed. Kaplan-Meier and log-rank tests were used for the OS analysis. Cox proportional hazards

regression models were used to assess risk factors for OS.  $p < 0.05$  indicated a statistically significant difference.

### 3. Results

#### 3.1. The regulation of *KCTD8* expression by DNA methylation

To assess the potential epigenetic regulation of *KCTD8* expression in HCC, the Cancer Genome Atlas (TCGA) database (<http://xena.ucsc.edu/>) was utilized. *KCTD8* mRNA and the methylation status of CpG sites around the transcription start site (TSS) were extracted from 115 cases of HCC. A significant inverse association was found between *KCTD8* expression and methylation of the promoter region (cg07650252,  $p = 0.0345$ ; cg12300353,  $p = 0.0053$ ; Figure 1A & B). Subsequently, *KCTD8* expression and promoter region methylation status were assessed using RT-PCR and MSP in HCC cells. Loss of *KCTD8* expression was found in Bel-7405, PLC/PRF5, HCCLM3, SNU449 and Huh7 cells, and complete methylation of the promoter region was observed in these cells. The expression of *KCTD8* was induced by 5-aza-2'-deoxycytidine (5-aza), a DNA methyltransferase (DNMT) inhibitor (Figure 1C & D). The afore mentioned findings suggest that *KCTD8* expression is regulated by methylation in the promoter region in HCC cells.

#### 3.2. Methylation of *KCTD8* was a poor prognostic marker in HCC

To evaluate the status of *KCTD8* methylation, MSP assay was utilized. It was observed that *KCTD8* was methylated in 44.83% (104/232) of HCC (Figure 1E). *KCTD8* methylation was significantly associated with TNM stage ( $p = 0.023$ ), while there was no significant association between *KCTD8* methylation and age, gender, tumor size, differentiation, metastasis of lymph node or liver cirrhosis (all  $p > 0.05$ , Table 1). For 117 cases of primary HCC with available follow-up data, 49 cases were methylated and 68 cases were unmethylated. The median age was 55 years old (range 29–71 years old), and the ratio of men to women was 6.31. The Kaplan-Meier model and Cox proportional hazards model were utilized to analyze the association of methylation with survival. In the *KCTD8* unmethylation group, the mean survival time was 52 months (95% CI 45–60 months), while in the *KCTD8* methylation group, the mean survival time was 34 months (95% CI 24–43 months). The OS was longer in *KCTD8* unmethylated patients than in methylated patients (Figure 1F,  $p = 0.0095$ ). *KCTD8* methylation was revealed to be an independent poor prognostic marker according to the multivariate analysis (Table 2,  $p = 0.041$ ).

#### 3.3. *KCTD8* suppressed HCC cell proliferation, colony formation, migration & invasion & induced apoptosis

To investigate the function of *KCTD8* in HCC, *KCTD8* stably expressed cells were established in *KCTD8* silenced Bel-7405 and PLC/PRF5 cells. MTT and colony formation assays were conducted to evaluate the role of *KCTD8* in cell proliferation. As shown in Figure 2A, the OD values of the *KCTD8* silenced and re-expressed Bel-7405 and PLC/PRF5 cells were  $0.919 \pm 0.027$  vs.  $0.721 \pm 0.034$  and  $0.934 \pm 0.033$  vs.  $0.675 \pm 0.033$ , respectively (both  $p < 0.0001$ ). The OD value was reduced significantly by re-expressing *KCTD8*, indicating that *KCTD8* inhibits cell proliferation. Without and with expression of *KCTD8* in these cells, the clone number was  $353 \pm 16$  vs.  $269 \pm 19$  and  $415 \pm 23$  vs.  $317 \pm 26$ , respectively (Figure 2B, both  $p < 0.01$ ). Clone number was decreased in *KCTD8* re-expressed Bel-7405 and PLC/PRF5 cells compared with unexpressed cells. These findings demonstrate that *KCTD8* exerts a suppressive effect on cell clonogenicity in HCC.

In Transwell assay, the migratory cells were  $249 \pm 32$  vs.  $110 \pm 31$  ( $p < 0.01$ ) in Bel-7405 cells and  $122 \pm 20$  vs.  $55 \pm 4$  ( $p < 0.01$ ) in PLC/PRF5 cells without and with *KCTD8* expression. A decreased number of migratory cells was observed by forced *KCTD8* expression (Figure 2C). For *KCTD8* silenced and forced expression cells, the number of invasive cells was  $173 \pm 14$  vs.  $64 \pm 20$  ( $p < 0.01$ ) in Bel-7405 cells and  $123 \pm 5$  vs.  $54 \pm 16$  ( $p < 0.01$ ) in PLC/PRF5 cells, respectively. Similarly, re-expression of *KCTD8* resulted in a reduction in the number of invasive cells, indicating the inhibitory role of *KCTD8* in cell invasion (Figure 2C). The levels of MMP2, MMP7 and MMP9, which are the migration and invasion related proteins, were examined. They were reduced by restoration of *KCTD8* expression in Bel-7405 and PLC/PRF5 cells, further suggesting that *KCTD8* suppresses cell migration and invasion (Figure 2D).

Flow cytometry technique was utilized to analyze the effect of *KCTD8* on apoptosis. The percentage was  $4.56 \pm 0.66\%$  vs.  $7.04 \pm 1.04\%$  ( $p < 0.05$ ) and  $4.01 \pm 0.16\%$  vs.  $8.06 \pm 0.23\%$  ( $p < 0.0001$ ) for apoptotic cells in *KCTD8* unexpressed and re-expressed Bel-7405 cells and PLC/PRF5 cells, respectively (Figure 2E). The molecular level of apoptosis-related proteins was examined. Increased levels of BAX and cleaved caspase-3 were observed in *KCTD8* over-expressed Bel-7405 and PLC/PRF5 cells, while the level of BCL-2 was reduced (Figure 2F), indicating that *KCTD8* induces apoptosis in HCC cells.



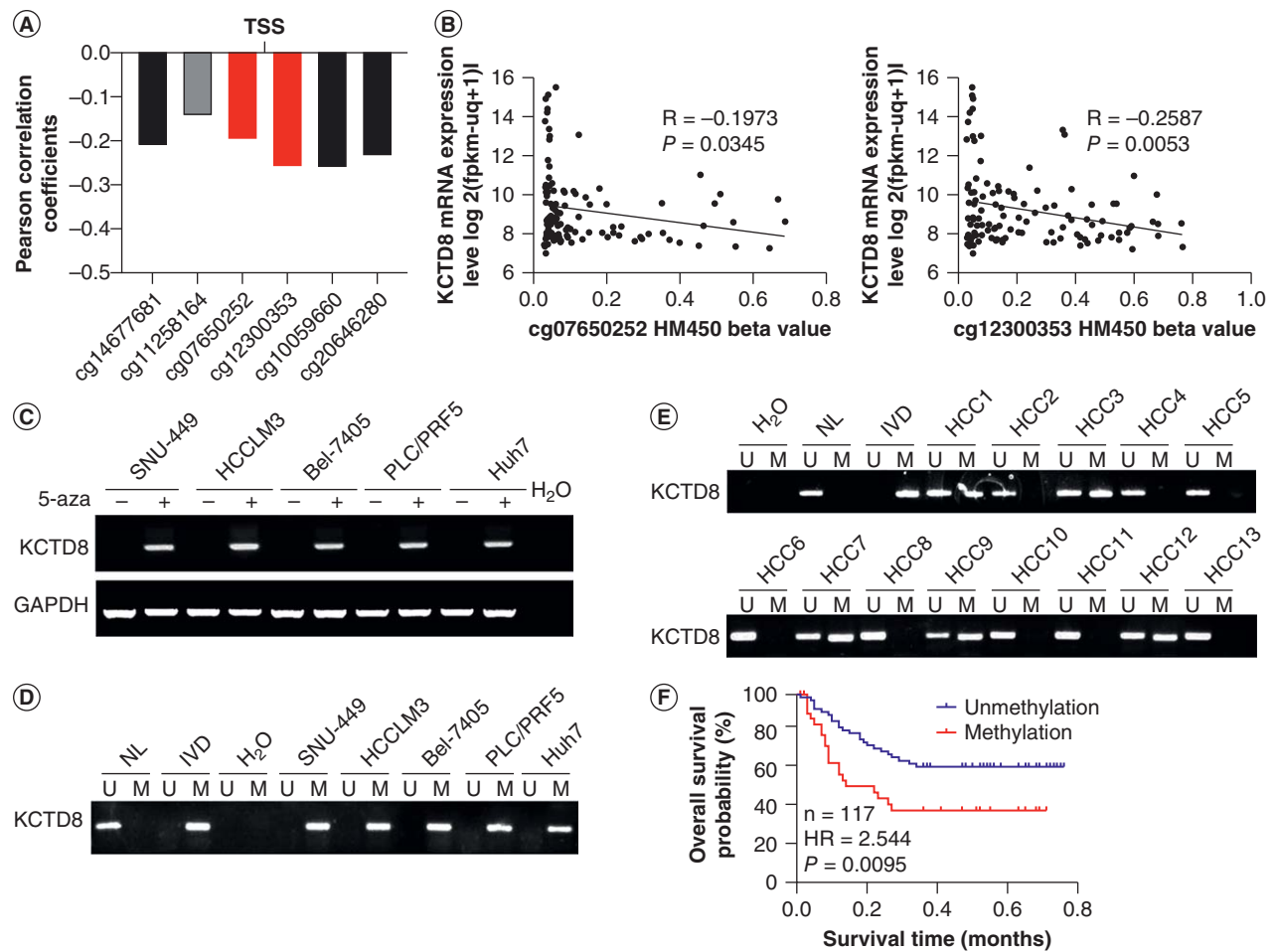


**Figure 1.** Representative results of KCTD8 expression and methylation status. **(A)** The association of KCTD8 mRNA level and methylation status of CpG sites around the TSS in HCC samples extracted from the TCGA database (n = 115). TSS: transcription start site. **(B)** Representative scatter plots for KCTD8 expression level and CpG sites methylation level (cg07650252, cg12300353). **(C)** Semi-quantitative RT-PCR showing the expression of KCTD8 in HCC cells before and after 5-aza treatment. 5-aza: 5-aza-2'-deoxycytidine; GAPDH: internal control for RT-PCR; H<sub>2</sub>O: double distilled water; (-): absence of 5-aza; (+): 5-aza treatment. **(D)** MSP results in HCC cells. MSP: methylation-specific polymerase chain reaction, U: unmethylated alleles; M: methylated alleles; IVD: *in vitro* methylated DNA, serves as methylation control; NL: normal lymphocytes DNA, serves as unmethylation control. **(E)** Representative MSP results in primary HCC. **(F)** Kaplan-Meier survival results showing the association between KCTD8 methylation and overall survival in HCC patients (n = 117, p = 0.0095).

### 3.4. KCTD8 interacted with IMPDH2 in Bel-7405 & PLC/PRF5 cells

The mechanism of KCTD8 in HCC was further explored with immunoprecipitation (IP) assay and mass spectrometry. An extra distinguishable band was excised for mass spectrometry analysis from KCTD8 re-expressed Bel-7405 cells (Figure 3A). Among the proteins in the complex pulled down by the KCTD8 antibody, IMPDH2 exhibited the highest score (Supplementary Table S1). Utilizing Co-IP and reciprocal Co-IP assay, the interaction of KCTD8 and IMPDH2 was further validated in both KCTD8 re-expressed Bel-7405 and PLC/PRF5 cells (Figure 3B).

### 3.5. KCTD8 inhibited PI3K/AKT signaling by interacting with IMPDH2

IMPDH2 has been found to play important roles in PI3K/AKT, Wnt signaling pathways and metabolism in human cancers [40–44]. To explore the possible signaling of KCTD8 involved in HCC cells, the proteins in the complex were analyzed. After excluding keratin and other cytoskeletal proteins, the remaining proteins were more frequently related to PI3K/AKT signaling pathway (Supplementary Table S1) [40–43,45–96]. Previous studies have demonstrated the interaction between KCTD8 and KCTD5, and KCTD5 was observed to inhibit PI3K/AKT

**Table 1.** Correlation of *KCTD8* methylation with clinic-pathological features of patients in HCC (n = 232).

Clinical parameter	No. 232	Methylation status		p-value
		Unmethylated n = 128 (55.12%)	Methylated n = 104 (44.83%)	
<b>Gender</b>				
Male	198	111	87	0.512
Female	34	17	17	
<b>Age</b>				
<60	151	87	64	0.307
≥60	81	41	40	
<b>Differentiation</b>				
Well/moderately	162	88	74	0.692
Poorly	70	40	30	
<b>TNM stage</b>				
I/II	97	62	35	0.023 <sup>a</sup>
III/IV	135	66	69	
<b>Lymph node metastasis</b>				
No	209	118	91	0.235
Yes	23	10	13	
<b>Tumor size</b>				
<5 cm	62	34	28	0.951
≥5 cm	170	94	76	
<b>Liver cirrhosis</b>				
No	59	33	26	0.892
Yes	173	95	78	

<sup>a</sup>p values are obtained from  $\chi^2$  test, significant difference.  
p < 0.05.

**Table 2.** Univariate and multivariate analysis of *KCTD8* methylation status with 5-year overall survival in HCC patients (n = 117).

Clinical parameter	Univariate analysis		Multivariate analysis	
	HR (95%CI)	p-value	HR (95%CI)	p-value
<b>Gender</b> (male vs. female)	1.017 (0.432,2.397)	0.969		
<b>Age</b> (≥60 vs. <60 years)	0.796 (0.426,1.489)	0.475		
<b>Tumor size</b> (≥5 vs. <5 cm)	1.540 (0.799,2.968)	0.197		
<b>Differentiation</b> (low vs. high or middle differentiation)	1.461 (0.816,2.616)	0.202		
<b>TNM stage</b> (III/IV vs. I/II)	2.925 (1.515,5.649)	0.001 <sup>b</sup>	2.704 (1.392,5.252)	0.003 <sup>b</sup>
<b>Lymph node metastasis</b> (Yes vs. No)	2.074 (0.642,6.699)	0.222		
<b>KCTD8</b> (methylation vs. unmethylation)	2.087 (1.171,3.718)	0.013 <sup>a</sup>	1.837 (1.025,3.293)	0.041 <sup>a</sup>
<b>Liver cirrhosis</b> (Yes vs. No)	1.024 (0.521,2.012)	0.946		

<sup>a</sup>p < 0.05.

<sup>b</sup>p < 0.01.

HR: Hazard ratio.

signaling [37,38]. Therefore, we focused on the PI3K/AKT signaling. Reduced levels of PI3K110 $\beta$ , p-AKT and p-mTOR were observed with *KCTD8* forced expression in Bel-7405 and PLC/PRF5 cells compared with unexpressed cells, indicating the inhibitory role of *KCTD8* in PI3K/AKT signaling (Figure 3C & D). To further validate the effect of *KCTD8* on PI3K/AKT pathway, NVP-BE2235, a dual inhibitor of PI3K/mTOR was used. Before and after treatment with NVP-BE2235, the OD values were  $0.797 \pm 0.024$  vs.  $0.670 \pm 0.020$  ( $p < 0.0001$ ) and  $0.881 \pm 0.034$  vs.  $0.754 \pm 0.008$  ( $p < 0.0001$ ) in *KCTD8* unexpressed Bel-7405 and PLC/PRF5 cells, respectively (Figure 3E). Without and with NVP-BE2235 treatment, the OD values were  $0.656 \pm 0.015$  vs.  $0.651 \pm 0.018$  ( $p > 0.05$ ) and  $0.732 \pm 0.019$  vs.  $0.710 \pm 0.028$  ( $p > 0.05$ ) in *KCTD8*

re-expressed Bel-7405 and PLC/PRF5 cells, respectively (Figure 3E). These findings provided more evidence for the inhibitory function of *KCTD8* in PI3K/AKT signaling. These results were validated by detecting the major components at the protein level. After treatment with NVP-BE2235, the levels of PI3K110 $\beta$ , p-AKT and p-mTOR were decreased in *KCTD8* silenced Bel-7405 and PLC/PRF5 cells, whereas without obvious changes in *KCTD8* re-expressed cells (Figure 3F & G).

To clarify the inhibitory role of *KCTD8* on PI3K/AKT/mTOR signaling through IMPDH2, siRNA knockdown technique was employed. The knockdown efficiency of siRNA was shown in Figure 3H & I. In *KCTD8* methylation silenced HCC cells, PI3K110 $\beta$ , p-AKT and p-mTOR were decreased by knocking down IMPDH2, while

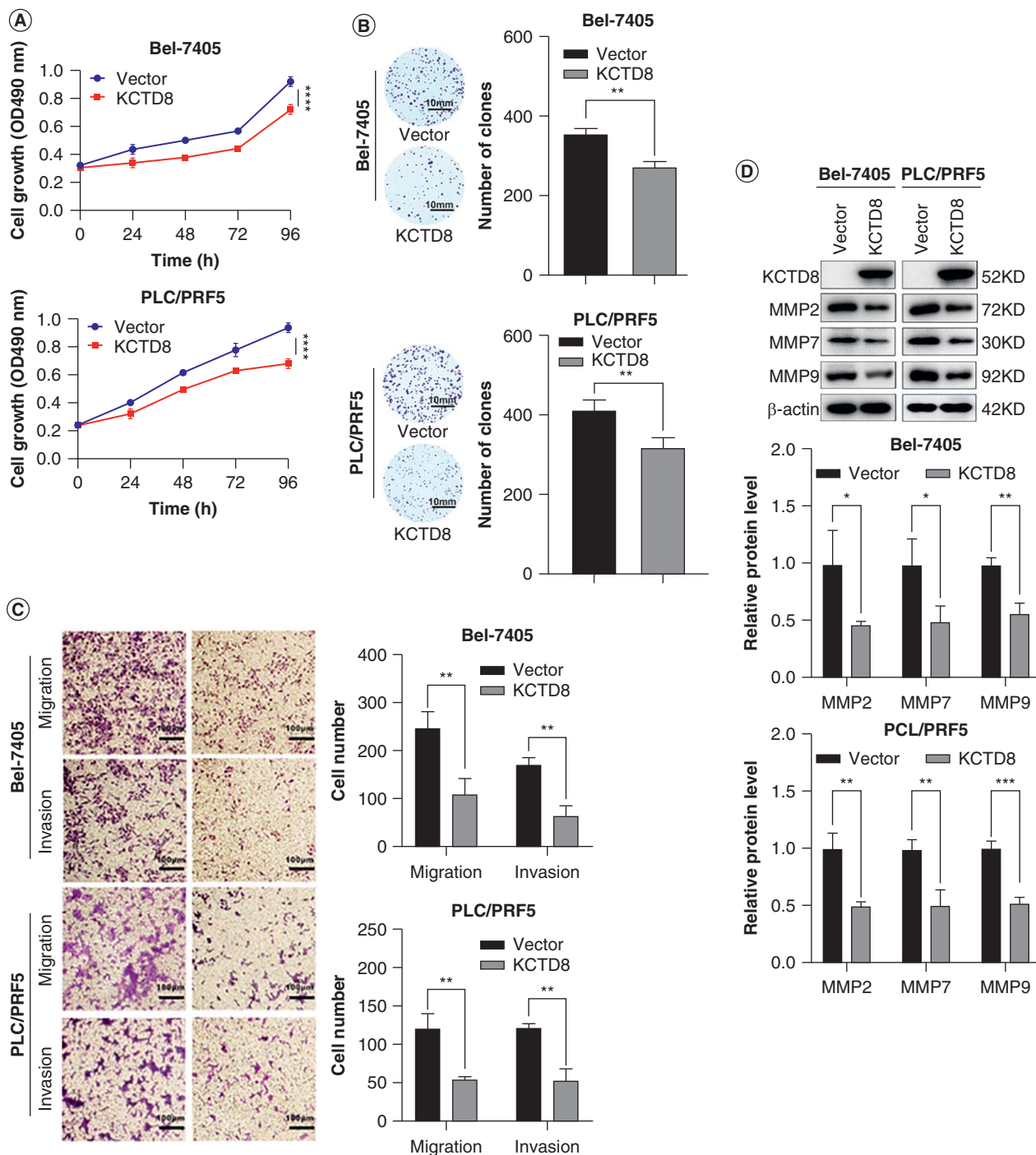


**Figure 2.** The effect of KCTD8 on cell proliferation, migration, invasion and apoptosis. **(A)** MTT assay showing the effect of KCTD8 on the cell proliferation of Bel-7405 and PLC/PRF5 cells. **(B)** Effect of KCTD8 on colony formation in Bel-7405 and PLC/PRF5 cells. The average number of clones was represented by the bar diagram. Scale: 10 mm. **(C)** Transwell assay showing the effect of KCTD8 on cell migration and invasion for Bel-7405 and PLC/PRF5 cells. The average number of migration cells was presented by a bar diagram. Scale: 100  $\mu$ m. **(D)** western blots showing the levels of MMP2, MMP7 and MMP9 in KCTD8 unexpressed and re-expressed HCC cells.  $\beta$ -actin served as control. The histogram showing the statistical analysis of the indicated relative protein expression level. **(E)** Flow cytometry assay showing the effect of KCTD8 on apoptosis in HCC cells. The average percentage of apoptotic cell was presented by a bar diagram. **(F)** The levels of caspase-3, cleaved caspase-3, BAX and BCL-2 in KCTD8 unexpressed and over-expressed cells. The histogram showing the statistical analysis of the indicated relative protein expression level. ns: no significance. Each experiment was repeated in triplicate. \* $p < 0.05$ ; \*\* $p < 0.01$ ; \*\*\* $p < 0.001$ ; \*\*\*\* $p < 0.0001$ .

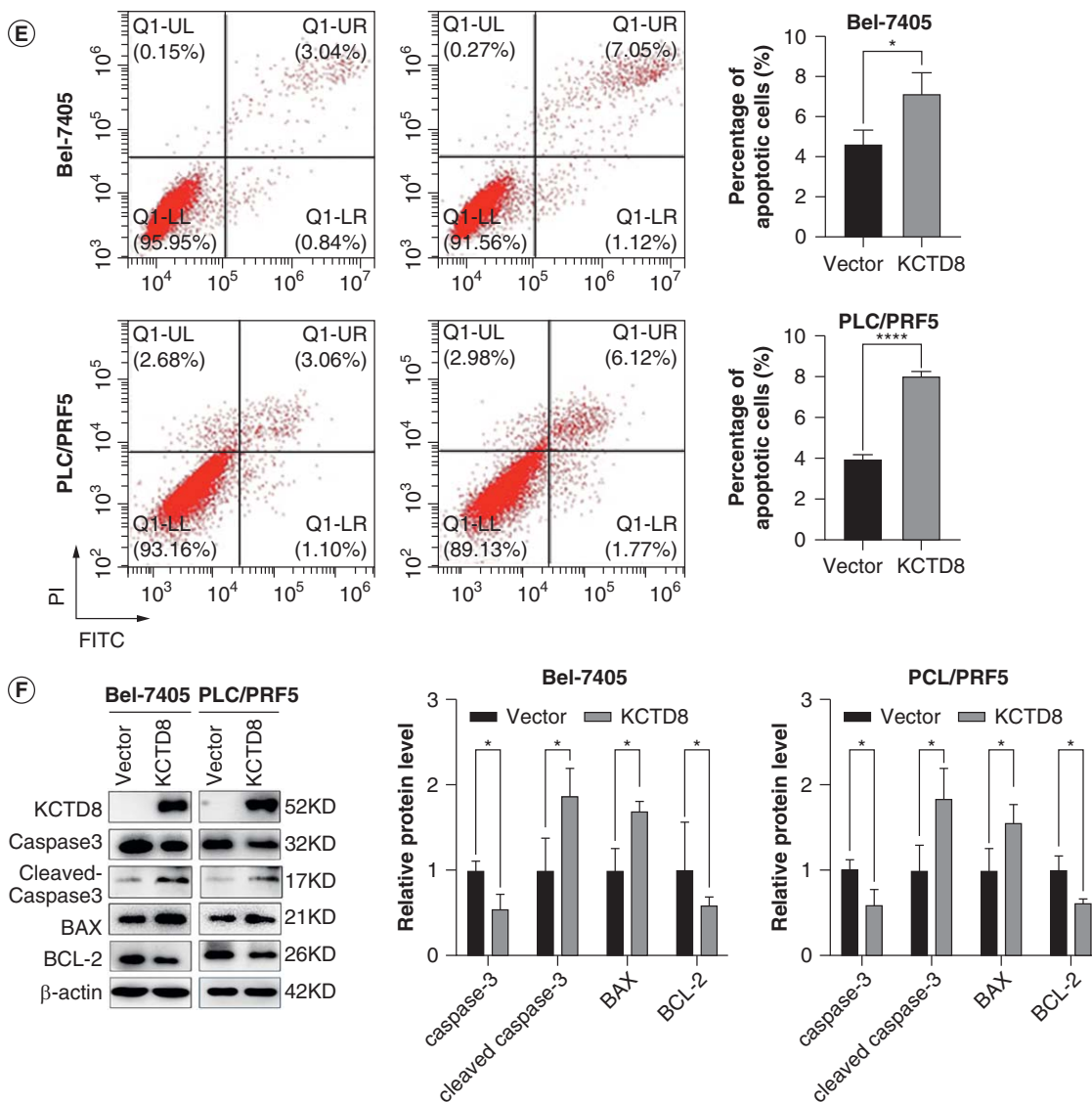


**Figure 2.** The effect of KCTD8 on cell proliferation, migration, invasion and apoptosis. **(A)** MTT assay showing the effect of KCTD8 on the cell proliferation of Bel-7405 and PLC/PRF5 cells. **(B)** Effect of KCTD8 on colony formation in Bel-7405 and PLC/PRF5 cells. The average number of clones was represented by the bar diagram. Scale: 10 mm. **(C)** Transwell assay showing the effect of KCTD8 on cell migration and invasion for Bel-7405 and PLC/PRF5 cells. The average number of migration cells was presented by a bar diagram. Scale: 100  $\mu$ m. **(D)** western blots showing the levels of MMP2, MMP7 and MMP9 in KCTD8 unexpressed and re-expressed HCC cells.  $\beta$ -actin served as control. The histogram showing the statistical analysis of the indicated relative protein expression level. **(E)** Flow cytometry assay showing the effect of KCTD8 on apoptosis in HCC cells. The average percentage of apoptotic cell was presented by a bar diagram. **(F)** The levels of caspase-3, cleaved caspase-3, BAX and BCL-2 in KCTD8 unexpressed and over-expressed cells. The histogram showing the statistical analysis of the indicated relative protein expression level. ns: no significance. Each experiment was repeated in triplicate (cont.).

\* $p < 0.05$ ; \*\* $p < 0.01$ ; \*\*\* $p < 0.001$ ; \*\*\*\* $p < 0.0001$ .

no obvious change was found in KCTD8 re-expressed cells (Figure 3J & K). No obvious changes in the total levels of AKT or mTOR were observed whether IMPDH2 was knocked down or not. The results suggest that KCTD8 inhibits PI3K/AKT/mTOR signaling pathway by interacting with IMPDH2.

### 3.6. KCTD8 suppressed BEL-7405 cell xenografts growth

The function of KCTD8 *in vivo* was investigated by employing xenograft mice. The tumor volume was  $656.28 \pm 104.44 \text{ mm}^3$  vs.  $116.62 \pm 44.30 \text{ mm}^3$  (Figure 4B,  $p < 0.0001$ ) and the tumor weight was  $0.24 \pm 0.03 \text{ g}$



vs.  $0.05 \pm 0.01$  g (Figure 4C,  $p < 0.0001$ ), before and after re-expressing KCTD8 in BEL-7405 cells. The tumor volume and weight were reduced significantly by expressing KCTD8. Additionally, immunohistochemistry staining showed reduced levels of PI3K110 $\beta$ , p-AKT, p-mTOR and ki67 by re-expressing KCTD8 in xenograft tumors (Figure 4D & E), demonstrating the inhibitory effect of KCTD8 on PI3K/AKT signaling *in vivo*.

## 4. Discussion

With the exhaustion of genomic resources, it is necessary to dig the mechanism of cancer-related signaling regulation and to widen the application of DNA and protein modifications in the field of precision medicine. Epigenetic dysregulation has been regarded as one of the major causes of cancer initiation and progression [18,97–99]. Epigenetic drugs (epi-drugs) have been

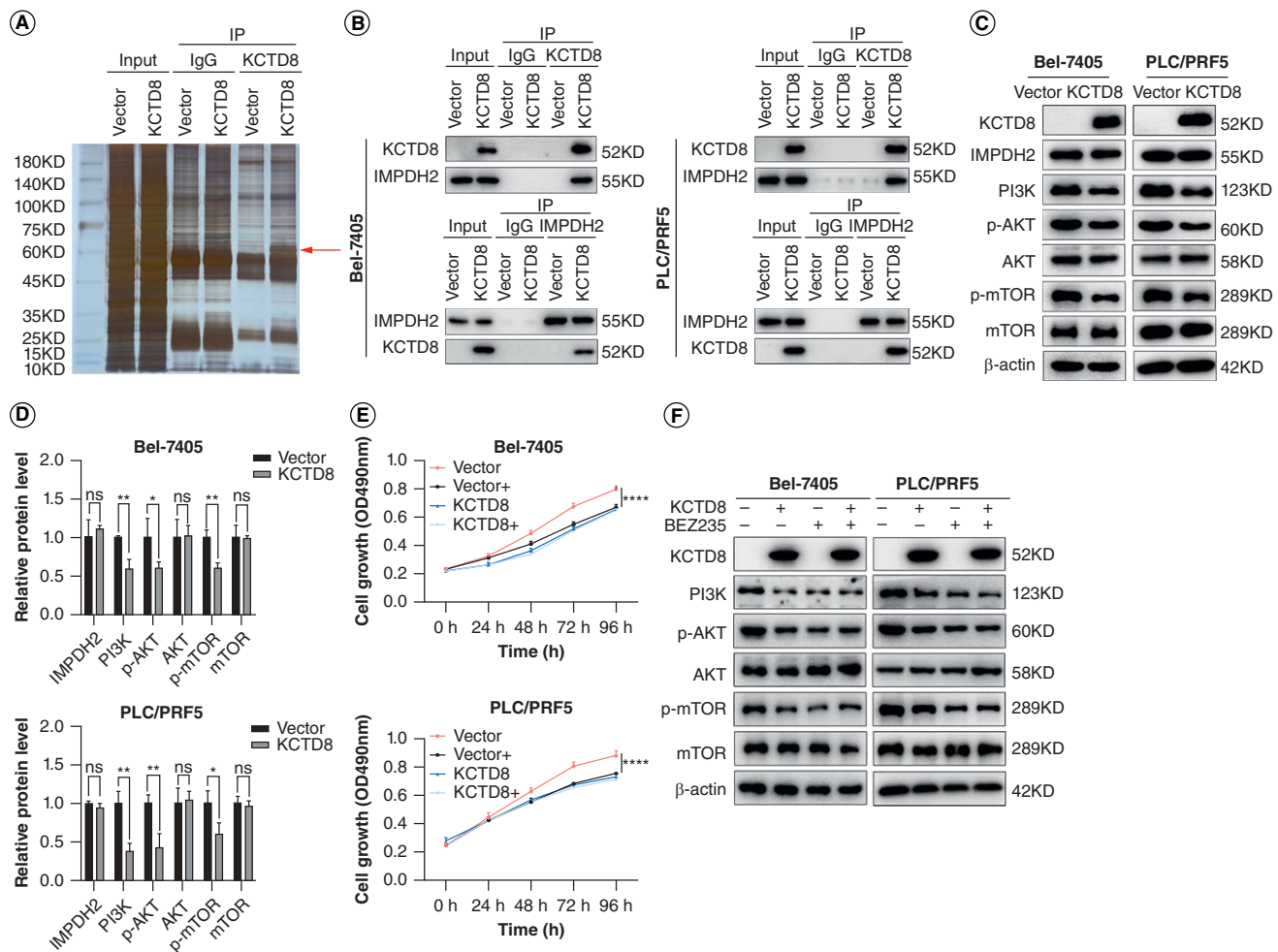


**Figure 3.** KCTD8 suppresses PI3K/AKT pathway by interacting with IMPDH2. **(A)** Polyacrylamide gel showing the results of immunoprecipitation with KCTD8 antibodies in Bel-7405 cells. The red arrow showing the distinct band in KCTD8 expressed cells. **(B)** IMPDH2 was validated to be the binding protein of KCTD8 by Co-IP (Up) and reciprocal Co-IP (down). **(C)** The levels of IMPDH2, PI3K110 $\beta$ , p-AKT, AKT, p-mTOR and mTOR in KCTD8 unexpressed and re-expressed HCC cells. **(D)** The histogram showing the statistical analysis of the relative protein expression level in **(C)**. **(E)** MTT assay showing the effects of KCTD8 and NVP-BE2235 on the cell proliferation of HCC cells. NVP-BE2235: a dual PI3K/mTOR inhibitor; Vector: KCTD8 unexpressed control cells; Vector+: KCTD8 unexpressed control cells treated with NVP-BE2235 (10 nM); KCTD8: KCTD8 over-expressed cells; KCTD8+: KCTD8 over-expressed cells treated with NVP-BE2235. **(F)** western blot showing the levels of PI3K110 $\beta$ , p-AKT, AKT, p-mTOR and mTOR in NVP-BE2235 treated and untreated HCC cells. **(G)** The histogram showing the statistical analysis of the indicated relative protein expression level in **(F)**. **(H)** western blot showing the efficiency of siRNA for IMPDH2 knockdown. Scrambled: siRNA negative control; siRNA#1, siRNA#2 and siRNA#3: siRNA for IMPDH2. **(I)** The histogram showing the statistical analysis of the relative IMPDH2 expression level after knockdown. **(J)** The levels of PI3K110 $\beta$ , p-AKT, AKT, p-mTOR and mTOR before and after transfection with siIMPDH2#3. **(K)** The histogram showing the statistical analysis of the indicated relative protein expression level in **(J)**. ns: no significance. Each experiment was repeated in triplicate.

\* $p < 0.05$ ; \*\* $p < 0.01$ ; \*\*\* $p < 0.001$ .

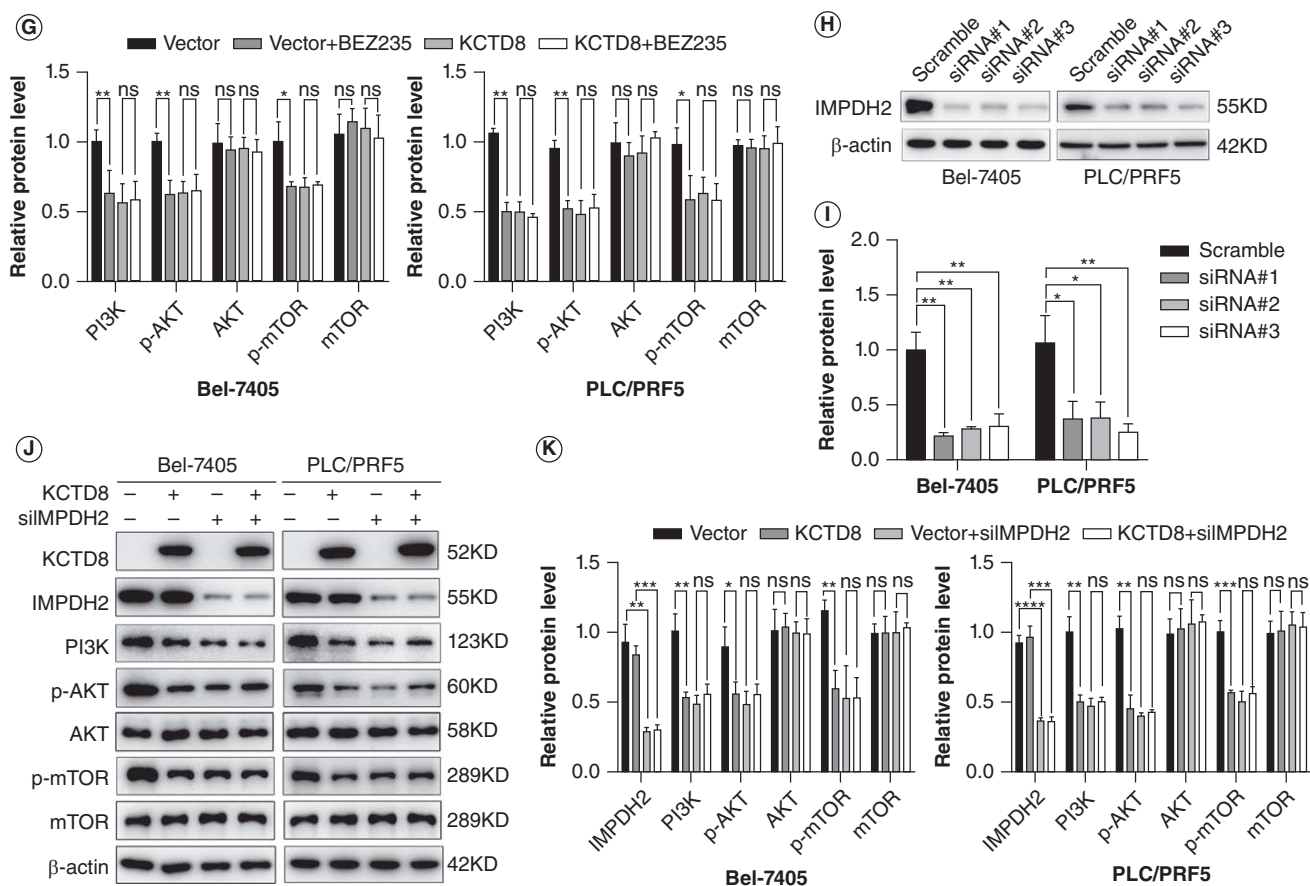


**Figure 3.** KCTD8 suppressed PI3K/AKT pathway by interacting with IMPDH2. **(A)** Polyacrylamide gel showing the results of immunoprecipitation with KCTD8 antibodies in Bel-7405 cells. The red arrow showing the distinct band in KCTD8 expressed cells. **(B)** IMPDH2 was validated to be the binding protein of KCTD8 by Co-IP (Up) and reciprocal Co-IP (down). **(C)** The levels of IMPDH2, PI3K110 $\beta$ , p-AKT, AKT, p-mTOR and mTOR in KCTD8 unexpressed and re-expressed HCC cells. **(D)** The histogram showing the statistical analysis of the relative protein expression level in **(C)**. **(E)** MTT assay showing the effects of KCTD8 and NVP-BE2325 on the cell proliferation of HCC cells. Vector: KCTD8 unexpressed control cells; Vector +: KCTD8 unexpressed control cells treated with NVP-BE2325 (10 nM); KCTD8: KCTD8 over-expressed cells; KCTD8+: KCTD8 over-expressed cells treated with NVP-BE2325. **(F)** western blot showing the levels of PI3K110 $\beta$ , p-AKT, AKT, p-mTOR and mTOR in NVP-BE2325 treated and untreated HCC cells. **(G)** The histogram showing the statistical analysis of the indicated relative protein expression level in **(F)**. **(H)** western blot showing the efficiency of siRNA for IMPDH2 knockdown. Scrambled: siRNA negative control; siRNA#1, siRNA#2 and siRNA#3: siRNA for IMPDH2. **(I)** The histogram showing the statistical analysis of the relative IMPDH2 expression level after knockdown. **(J)** The levels of PI3K110 $\beta$ , p-AKT, AKT, p-mTOR and mTOR before and after transfection with siIMPDH2#3. **(K)** The histogram showing the statistical analysis of the indicated relative protein expression level in **(J)**. ns: no significance. Each experiment was repeated in triplicate (cont.).

\* $p < 0.05$ ; \*\* $p < 0.01$ ; \*\*\* $p < 0.001$ .

developed to target regulatory enzymes, including writer (addition of modifications to DNA or histone), reader (recognition of epigenetic modifications) and eraser (removal of DNA or histone modifications) [21,22,100]. The most extensively tested epi-drugs are DNMTs and histone deacetylase (HDAC) inhibitors. As imprecisely targeting tumor cells, these drugs are mainly confined to hematological cancers, and have very limited efficacy against solid tumors [23,98]. It is desirable to deeper understand the role of epigenetic regulation in tumor-related signaling and discover novel abnormal modifications of components in these pathways to develop novel

therapeutic strategies. Epigenetic silencing of zinc-finger protein *ZFP82* promoted esophageal cancer cell growth by activating NF- $\kappa$ B signaling pathway [101]. Methylation of *ZNF377* inhibited pyroptosis in multiple types of cancer cell lines and paved the way for cancer therapy [102]. Epigenetic silencing of *JAM3* or *ZSCAN23* activated Wnt signaling pathway in different cancers [103,104]. Targeting cell fate determining signaling pathways or its compensatory pathways may develop new therapeutic approaches, by utilizing the epigenetic abnormality in cancer [23]. Epigenetic silencing tumor suppressors and dysregulating their related signaling pathways have been

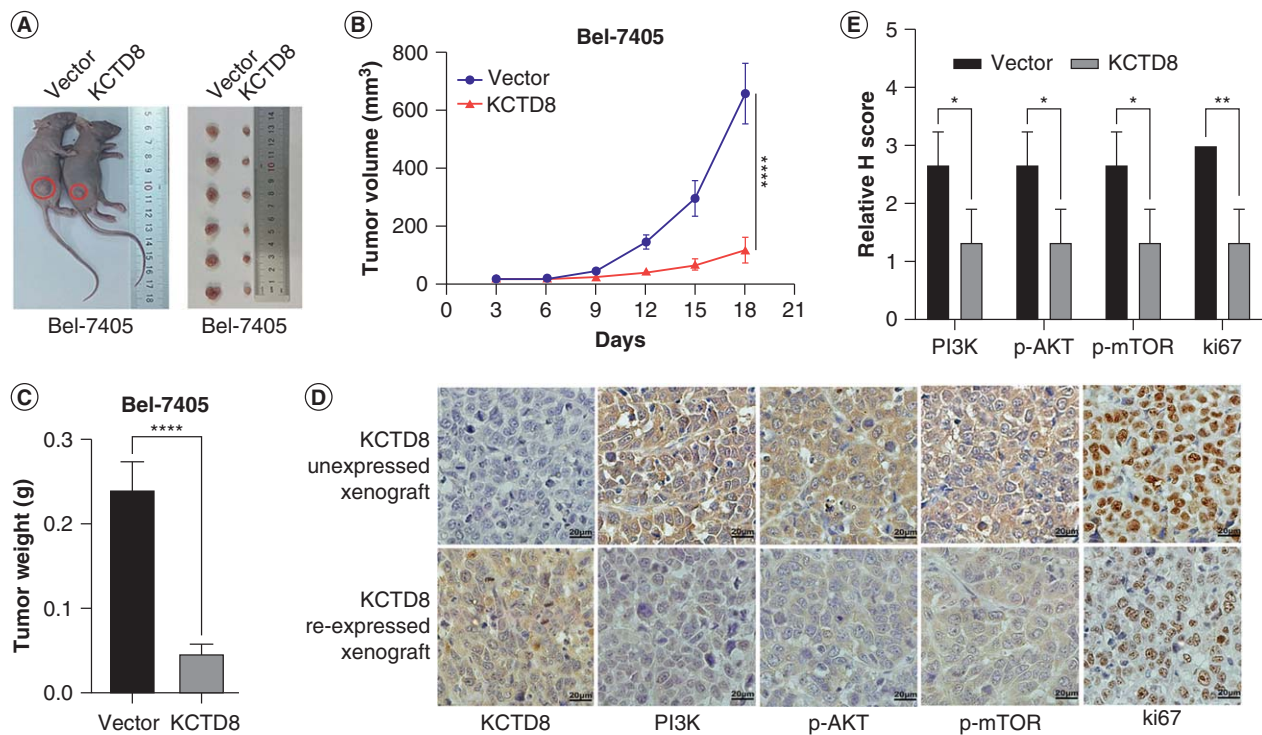


**Figure 4.** The role of KCTD8 in xenograft mice model. **(A)** Xenograft tumors of KCTD8 unexpressed and re-expressed Bel-7405 cells. **(B)** Growth curves showing the xenograft volumes of KCTD8 silenced and over-expressed Bel-7405 cells. **(C)** Bar graph representing the tumor weight of xenografts in KCTD8 silenced and over-expressed Bel-7405 cells. **(D)** Representative IHC results of KCTD8, PI3K, p-AKT, p-mTOR and ki67 in xenografts. Scale: 20 μm. **(E)** The histogram showing relative expression level of the indicated relative markers in xenografts by H score.

\* $p < 0.05$ ; \*\* $p < 0.01$ ; \*\*\*\* $p < 0.0001$ .

reported in HCC. However, the biological roles of tumor-related genes vary depending on their surrounding microenvironment [105]. Unlike other tumors, epigenetic changes were not well studied in HCC. The researches on epigenomic landscape in HCC are very limited [22,106]. To find novel tumor suppressor and further understand the mechanisms in HCC may provide more opportunities for its treatment. The character of KCTD8 was not explored in HCC. In the present investigation, a high frequency of KCTD8 methylation and the regulatory role of DNA methylation were observed. KCTD8 methylation was associated with TNM stage and poor OS, suggesting that epigenetic regulation of KCTD8 is involved in HCC progression. To further elucidate the mechanism of KCTD8, the biological function was investigated in HCC cells. Our findings demonstrated that KCTD8 exerted inhibitory role in cancer development *in vitro* and suppressed HCC cell xenografts growth in mice, implicating that KCTD8 may act as a tumor suppressor in HCC. Co-IP and mass spectrometry assays were employed to clarify the mechanism of KCTD8. The interaction of KCTD8 and IMPDH2 was identified and further validated by western blot and reciprocal IP assay. Notably, IMPDH2 is reported to be involved in the PI3K signaling pathway.

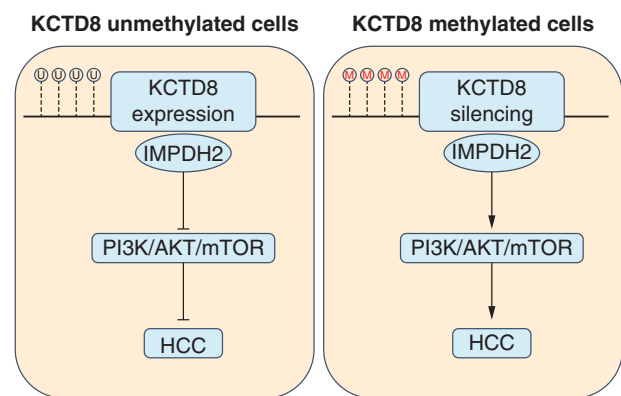


**Figure 5.** The schematic graphic illustrating that epigenetic silencing of KCTD8 activated PI3K/AKT signaling in HCC. M: Methylation; U: Unmethylation.

Then, the role of KCTD8 in PI3K signaling was explored in HCC. The results showed that KCTD8 inhibited PI3K signaling both *in vitro* and *in vivo*. As shown in Graphical Abstract (Figure 5), PI3K signaling was inhibited by KCTD8 interacting with IMPDH2, it was activated by IMPDH2 after epigenetic silencing of KCTD8.

The function of PI3K signaling pathway is very complex. It involves in cell proliferation, apoptosis, chemo-

resistance, DDR and other biological behaviors [107]. In various cancers, PI3K signaling may join distinct regulatory networks through crosstalk under the different circumstance [108–110]. Therefore, it is crucial to comprehensively analyze the gene regulatory networks in HCC to develop new therapeutic approaches. Our results pave the way for precision medicine in HCC.

Utilizing abnormal epigenetic events for cancer therapy has been becoming an important topic. The application of synthetic lethality principle has revolutionized cancer therapeutic strategy, killing cancer cells specifically, without hurting normal cell [23,111]. Epigenetic regulation of key components in different signaling pathways makes epigenetic defects more important for precision medicine, including cell fate and DNA damage repair genes [21]. The precise cancer DNA methylome is still waiting for completion. Finding key components in these pathways and deep understanding their roles, as well as epigenetic regulation, may offer more opportunities for epigenetic-based synthetic lethality strategy.

## 5. Conclusion

In summary, our findings revealed the regulatory role of DNA methylation in KCTD8 expression. Methylation of *KCTD8* was a potential independent poor prognostic marker in HCC. *KCTD8* suppressed HCC by inhibiting PI3K/AKT pathway *in vitro* and *in vivo*.

### Article highlights

- Epigenetic dysregulation is a new hallmark for cancer therapy.
- Classical epi-drugs are mainly targeting epigenetic regulators, without tumor cell specificity.
- Deep understanding the role of epigenetic regulation in cancer-related signaling pathways may provide novel therapeutic targets.
- *KCTD8* is frequently methylated in HCC.
- *KCTD8* methylation is an independent poor prognostic biomarker in HCC.
- *KCTD8* inhibits HCC cells growth both *in vitro* and *in vivo*.
- Epigenetic silencing of *KCTD8* activates PI3K/AKT signaling pathway in HCC.
- *KCTD8* is a novel tumor suppressor in HCC.

## Author contributions

M Guo designed the research study and provided the funding support. J Zhou and M Zhang performed the research. J Zhou and A Gao analyzed the data. J Zhou and M Guo wrote the manuscript. JG Herman and M Guo interpreted the data and revised the manuscript. All authors contributed to editorial changes in the manuscript. All authors read and approved the final manuscript.

## Financial disclosure

This study was supported by grants from the National Key Research and Development Program of China (NO.

2020YFC2002705); National Natural Science Foundation of China (NO. 82272632, NO. 81672318); Youth Innovation Science Foundation of Chinese PLA general hospital (No. 22QNCZ027). The authors have no other relevant affiliations or financial involvement with any organization or entity with a financial interest in or financial conflict with the subject matter or materials discussed in the manuscript apart from those disclosed.

## Competing interests disclosure

The authors have no competing interests or relevant affiliations with any organization or entity with the subject matter or materials discussed in the manuscript. This includes employment, consultancies, honoraria, stock ownership or options, expert testimony, grants or patents received or pending, or royalties.

## Writing disclosure

No writing assistance was utilized in the production of this manuscript.

## Ethical conduct of research

This study was in accordance with the principles of the Declaration of Helsinki and was approved by the Institutional Review Board of the Chinese PLA General Hospital (IRB number: 20090701-015). Informed consents involving human subjects were obtained from all the participants. All the animal experiment protocols were performed according to the Animal Ethics Committee at Chinese PLA General Hospital (approval number: 2022-X18-72).

## Data availability statement

Data that supports the findings of this study are available from the corresponding author upon reasonable request.

## ORCID

Jing Zhou  <https://orcid.org/0009-0009-7481-2435>  
 Meiyong Zhang  <https://orcid.org/0009-0007-8990-7889>  
 Aiai Gao  <https://orcid.org/0009-0004-7006-5819>  
 James G Herman  <https://orcid.org/0000-0001-8102-1740>  
 Mingzhou Guo  <https://orcid.org/0000-0002-9445-9984>

## References

Papers of special note have been highlighted as: ● of interest; ●● of considerable interest

1. Sung H, Ferlay J, Siegel RL, et al. Global Cancer Statistics 2020: GLOBOCAN Estimates of Incidence and Mortality Worldwide for 36 Cancers in 185 Countries. *CA Cancer J Clin.* 2021;71(3):209–249. doi:10.3322/caac.21660
2. Villanueva A. Hepatocellular carcinoma. *New England J Med.* 2019;380(15):1450–1462. doi:10.1056/NEJMra1713263
3. Younossi Z, Stepanova M, Ong JP, et al. Nonalcoholic steatohepatitis is the fastest growing cause of hepatocellular carcinoma in liver transplant candidates. *Clin Gastroenterol Hepatol.* 2019;17(4):748–755.e3. doi:10.1016/j.cgh.2018.05.057



4. Zehir A, Benayed R, Shah RH, et al. Mutational landscape of metastatic cancer revealed from prospective clinical sequencing of 10,000 patients. *Nat Med.* 2017;23(6):703–713. doi:10.1038/nm.4333
5. Llovet JM, Montal R, Sia D, et al. Molecular therapies and precision medicine for hepatocellular carcinoma. *Nat Rev Clin Oncol.* 2018;15(10):599–616. doi:10.1038/s41571-018-0073-4
6. Chen L, Zhang C, Xue R, et al. Deep whole-genome analysis of 494 hepatocellular carcinomas. *Nature.* 2024;627(8004):586–593. doi:10.1038/s41586-024-07054-3
- **Whole-genome sequence in hepatocellular carcinomas.**
7. Llovet JM, Pinyol R, Kelley RK, et al. Molecular pathogenesis and systemic therapies for hepatocellular carcinoma. *Nat Cancer.* 2022;3(4):386–401. doi:10.1038/s43018-022-00357-2
- **Advancement in hepatocellular carcinomas therapy.**
8. Yarchoan M, Agarwal P, Villanueva A, et al. Recent developments and therapeutic strategies against hepatocellular carcinoma. *Cancer Res.* 2019;79(17):4326–4330. doi:10.1158/0008-5472.CAN-19-0803
9. Wang Y, Deng B. Hepatocellular carcinoma: molecular mechanism, targeted therapy, and biomarkers. *Cancer Metast Rev.* 2023;42(3):629–652. doi:10.1007/s10555-023-10084-4
10. Feng GS. Conflicting roles of molecules in hepatocarcinogenesis: paradigm or paradox. *Cancer Cell.* 2012;21(2):150–154. doi:10.1016/j.ccr.2012.01.001
11. Malone ER, Oliva M, Sabatini PJB, et al. Molecular profiling for precision cancer therapies. *Genom Med.* 2020;12(1):8. doi:10.1186/s13073-019-0703-1
12. Ma K, Cao B, Guo M. The detective, prognostic, and predictive value of DNA methylation in human esophageal squamous cell carcinoma. *Clin Epigenet.* 2016;8:43. doi:10.1186/s13148-016-0210-9
13. Heilbron K, Mozaffari SV, Vacic V, et al. Advancing drug discovery using the power of the human genome. *J Pathol.* 2021;254(4):418–429. doi:10.1002/path.5664
14. Hahn WC, Bader JS, Braun TP, et al. An expanded universe of cancer targets. *Cell.* 2021;184(5):1142–1155. doi:10.1016/j.cell.2021.02.020
- **The extension of targeting therapy.**
15. Chang L, Ruiz P, Ito T, et al. Targeting pan-essential genes in cancer: challenges and opportunities. *Cancer Cell.* 2021;39(4):466–479. doi:10.1016/j.ccell.2020.12.008
- **The Challenge of precision medicine**
16. Dupont CA, Riegel K, Pompaiah M, et al. Druggable genome and precision medicine in cancer: current challenges. *FEBS J.* 2021;288(21):6142–6158. doi:10.1111/febs.15788
17. Schaub FX, Dhankani V, Berger AC, et al. Pan-cancer alterations of the MYC oncogene and its proximal network across the cancer genome atlas. *Cell Syst.* 2018;6(3):282–300.e2. doi:10.1016/j.cels.2018.03.003
18. Guo M, Peng Y, Gao A, et al. Epigenetic heterogeneity in cancer. *Biomark Res.* 2019;7:23. doi:10.1186/s40364-019-0174-y
- **The epigenetic heterogeneity in cancer.**
19. Gupta P, Zhao H, Hoang B, et al. Targeting the untar-getable: RB1-deficient tumours are vulnerable to Skp2 ubiquitin ligase inhibition. *Br J Cancer.* 2022;127(6):969–975. doi:10.1038/s41416-022-01898-0
20. Molica S, Tam C, Allsup D, et al. Targeting TP53 disruption in chronic lymphocytic leukemia: current strategies and future directions. *Hematol Oncol.* 2024;42(1):e3238. doi:10.1002/hon.3238
21. Yan W, Herman JG, Guo M. Epigenome-based personalized medicine in human cancer. *Epigenomics.* 2016;8(1):119–133. doi:10.2217/epi.15.84
22. Miranda Furtado CL, Dos Santos Luciano MC, Silva Santos RD, et al. Epidrugs: targeting epigenetic marks in cancer treatment. *Epigenetics.* 2019;14(12):1164–1176. doi:10.1080/15592294.2019.1640546
23. Gao A, Guo M. Epigenetic based synthetic lethal strategies in human cancers. *Biomark Res.* 2020;8:44. doi:10.1186/s40364-020-00224-1
- **Epigenetic based synthetic lethality.**
24. Hu Y, Guo M. Synthetic lethality strategies: beyond BRCA1/2 mutations in pancreatic cancer. *Cancer Sci.* 2020;111(9):3111–3121. doi:10.1111/cas.14565
25. Gao A, Bai P, Zhang M, et al. RASSF1A promotes ATM signaling and RASSF1A methylation is a synthetic lethal marker for ATR inhibitors. *Epigenomics.* 2023;15(22):1205–1220. doi:10.2217/epi-2023-0306
26. Du W, Gao A, Herman JG, et al. Methylation of NRN1 is a novel synthetic lethal marker of PI3K-Akt-mTOR and ATR inhibitors in esophageal cancer. *Cancer Sci.* 2021;112(7):2870–2883. doi:10.1111/cas.14917
27. Angrisani A, Di Fiore A, De Smaele E, et al. The emerging role of the KCTD proteins in cancer. *Cell Comm Signal.* 2021;19(1):56. doi:10.1186/s12964-021-00737-8
28. Perez-Torrado R, Yamada D, Defossez PA. Born to bind: the BTB protein-protein interaction domain. *BioEssays.* 2006;28(12):1194–1202. doi:10.1002/bies.20500
29. Pinkas DM, Sanvitale CE, Bufton JC, et al. Structural complexity in the KCTD family of Cullin3-dependent E3 ubiquitin ligases. *Biochem J.* 2017;474(22):3747–3761. doi:10.1042/BCJ20170527
30. Stogios PJ, Downs GS, Jauhal JJ, et al. Sequence and structural analysis of BTB domain proteins. *Genome Biol.* 2005;6(10):R82. doi:10.1186/gb-2005-6-10-r82
31. Liu Z, Xiang Y, Sun G. The KCTD family of proteins: structure, function, disease relevance. *Cell Biosci.* 2013;3(1):45. doi:10.1186/2045-3701-3-45
32. Skoblov M, Marakhonov A, Marakasova E, et al. Protein partners of KCTD proteins provide insights about their functional roles in cell differentiation and vertebrate development. *BioEssays.* 2013;35(7):586–596. doi:10.1002/bies.201300002
33. Teng X, Aouacheria A, Lionnard L, et al. KCTD: a new gene family involved in neurodevelopmental and neuropsychiatric disorders. *CNS Neurosci Ther.* 2019;25(7):887–902. doi:10.1111/cns.13156
34. Fritzius T, Stawarski M, Isogai S, et al. Structural basis of GABA(B) receptor regulation and signaling. *Curr Topics Behav Neurosci.* 2022;52:19–37. doi:10.1007/7854\_2020\_147
35. Yao H, Ren D, Wang Y, et al. KCTD9 inhibits the Wnt/ $\beta$ -catenin pathway by decreasing the level of  $\beta$ -catenin in colorectal cancer. *Cell Death Dis.* 2022;13(9):761. doi:10.1038/s41419-022-05200-1

36. Ye RY, Kuang XY, Zeng HJ, et al. KCTD12 promotes G1/S transition of breast cancer cell through activating the AKT/FOXO1 signaling. *J Clin Lab Anal.* 2020;34(8):e23315. doi:10.1002/jcla.23315
37. Brockmann M, Blomen VA, Nieuwenhuis J, et al. Genetic wiring maps of single-cell protein states reveal an off-switch for GPCR signalling. *Nature.* 2017;546(7657):307–311. doi:10.1038/nature22376
38. Liao Y, Sloan DC, Widjaja JH, et al. KCTD5 forms heterooligomeric complexes with various members of the KCTD protein family. *Inter J Mol Sci.* 2023;24(18):14317. doi:10.3390/ijms241814317
39. Faryna M, Konermann C, Aulmann S, et al. Genome-wide methylation screen in low-grade breast cancer identifies novel epigenetically altered genes as potential biomarkers for tumor diagnosis. *FASEB J.* 2012;26(12):4937–4950. doi:10.1096/fj.12-209502
40. Xu H, Ma H, Zha L, et al. IMPDH2 promotes cell proliferation and epithelial-mesenchymal transition of non-small cell lung cancer by activating the Wnt/ $\beta$ -catenin signaling pathway. *Oncol Lett.* 2020;20(5):219. doi:10.3892/ol.2020.12082
41. Duan S, Huang W, Liu X, et al. IMPDH2 promotes colorectal cancer progression through activation of the PI3K/AKT/mTOR and PI3K/AKT/FOXO1 signaling pathways. *J Experiment Clin Cancer Res.* 2018;37(1):304. doi:10.1186/s13046-018-0980-3
42. Gao G, Xue Q, He J, et al. Single-cell RNA sequencing in double-hit lymphoma: IMPDH2 induces the progression of lymphoma by activating the PI3K/AKT/mTOR signaling pathway. *Int Immunopharmacol.* 2023;125(Pt A):111125. doi:10.1016/j.intimp.2023.111125
43. Bianchi-Smiraglia A, Wolff DW, Marston DJ, et al. Regulation of local GTP availability controls RAC1 activity and cell invasion. *Nat Commun.* 2021;12(1):6091. doi:10.1038/s41467-021-26324-6
44. Yuan H, Zhao Z, Xu J, et al. Hypoxia-induced TMTC3 expression in esophageal squamous cell carcinoma potentiates tumor angiogenesis through Rho GTPase/STAT3/VEGFA pathway. *J Experiment Clin Cancer Res.* 2023;42(1):249. doi:10.1186/s13046-023-02821-y
45. Kofuji S, Sasaki AT. GTP metabolic reprogramming by IMPDH2: unlocking cancer cells' fuelling mechanism. *J Biochem.* 2020;168(4):319–328. doi:10.1093/jb/mvaa085
46. Li TW, Kenney AD, Park JG, et al. SARS-CoV-2 Nsp14 protein associates with IMPDH2 and activates NF- $\kappa$ B signaling. *Front Immunol.* 2022;13:1007089. doi:10.3389/fimmu.2022.1007089
47. Lei YQ, Ye ZJ, Wei YL, et al. Nono deficiency impedes the proliferation and adhesion of H9c2 cardiomyocytes through Pi3k/Akt signaling pathway. *Scient Reports.* 2023;13(1):7134. doi:10.1038/s41598-023-32572-x
48. Lone BA, Siraj F, Sharma I, et al. Non-POU domain-containing octamer-binding (NONO) protein expression and stability promotes the tumorigenicity and activation of Akt/MAPK/ $\beta$ -catenin pathways in human breast cancer cells. *Cell Commun Sign.* 2023;21(1):157. doi:10.1186/s12964-023-01179-0
49. Kim SJ, Ju JS, Kang MH, et al. RNA-binding protein NONO contributes to cancer cell growth and confers drug resistance as a theranostic target in TNBC. *Theranostics.* 2020;10(18):7974–7992. doi:10.7150/thno.45037
50. de Silva HC, Lin MZ, Phillips L, et al. IGFBP-3 interacts with NONO and SFPQ in PARP-dependent DNA damage repair in triple-negative breast cancer. *Cell Mol Life Sci.* 2019;76(10):2015–2030. doi:10.1007/s00018-019-03033-4
51. Tanaka N, Chakravarty AK, Maughan B, et al. Novel mechanism of RNA repair by RtcB via sequential 2',3'-cyclic phosphodiesterase and 3'-Phosphate/5'-hydroxyl ligation reactions. *J Biolog Chem.* 2011;286(50):43134–43143. doi:10.1074/jbc.M111.302133
52. Akiyama Y, Takenaka Y, Kasahara T, et al. RTCB complex regulates stress-induced tRNA cleavage. *Inter JMol Sci.* 2022;23(21):13100. doi:10.3390/ijms232113100
53. He Z, Yang J, Sui C, et al. FAM98A promotes resistance to 5-fluorouracil in colorectal cancer by suppressing ferroptosis. *Arch Biochem Biophys.* 2022;722:109216. doi:10.1016/j.abb.2022.109216
54. Zheng R, Liu Q, Wang T, et al. FAM98A promotes proliferation of non-small cell lung cancer cells via the P38-ATF2 signaling pathway. *Cancer Manag Res.* 2018;10:2269–2278. doi:10.2147/CMAR.S163323
55. Liu S, Huang J, Zhang Y, et al. MAP2K4 interacts with Vimentin to activate the PI3K/AKT pathway and promotes breast cancer pathogenesis. *Aging.* 2019;11(22):10697–10710. doi:10.18632/aging.102485
56. Satelli A, Li S. Vimentin in cancer and its potential as a molecular target for cancer therapy. *Cell Mol Life Sci.* 2011;68(18):3033–3046. doi:10.1007/s00018-011-0735-1
57. Wang W, Chen H, Gao W, et al. Girdin interaction with vimentin induces EMT and promotes the growth and metastasis of pancreatic ductal adenocarcinoma. *Oncol Reports.* 2020;44(2):637–649. doi:10.3892/or.2020.7615
58. Cheng F, Shen Y, Mohanasundaram P, et al. Vimentin coordinates fibroblast proliferation and keratinocyte differentiation in wound healing via TGF- $\beta$ -Slug signaling. *Proc Natl Acad Sci USA.* 2016;113(30):E4320–4327. doi:10.1073/pnas.1519197113
59. Berr AL, Wiese K, Dos Santos G, et al. Vimentin is required for tumor progression and metastasis in a mouse model of non-small cell lung cancer. *Oncogene.* 2023;42(25):2074–2087. doi:10.1038/s41388-023-02703-9
60. van Engeland NCA, Suarez Rodriguez F, Rivero-Müller A, et al. Vimentin regulates Notch signaling strength and arterial remodeling in response to hemodynamic stress. *Scient Reports.* 2019;9(1):12415. doi:10.1038/s41598-019-48218-w
61. Antfolk D, Sjöqvist M, Cheng F, et al. Selective regulation of Notch ligands during angiogenesis is mediated by vimentin. *Proc Natl Acad Sci USA.* 2017;114(23):E4574–E4581. doi:10.1073/pnas.1703057114
62. Di Stefano B, Luo EC, Haggerty C, et al. The RNA helicase DDX6 controls cellular plasticity by modulating P-body homeostasis. *Cell Stem Cell.* 2019;25(5):622–638.e13. doi:10.1016/j.stem.2019.08.018
63. Balak C, Benard M, Schaefer E, et al. Rare *de novo* missense variants in RNA helicase DDX6 cause intellectual disability and dysmorphic features and lead to P-body defects and RNA dysregulation. *Am J Hum Genet.* 2019;105(3):509–525. doi:10.1016/j.ajhg.2019.07.010

64. Marcon BH, Rebelatto CK, Cofré AR, et al. DDX6 helicase behavior and protein partners in human adipose tissue-derived stem cells during early adipogenesis and osteogenesis. *InterJ Mol Sci.* 2020;21(7):2607. doi:10.3390/ijms21072607
65. Kato Y, Saga Y. Antagonism between DDX6 and PI3K-AKT signaling is an oocyte-intrinsic mechanism controlling primordial follicle growth. *Biol Reprod.* 2023;109(1):73–82. doi:10.1093/biolre/ioad043
66. Taniguchi K, Iwatsuki A, Sugito N, et al. Oncogene RNA helicase DDX6 promotes the process of c-Myc expression in gastric cancer cells. *Mol Carcinog.* 2018;57(5):579–589. doi:10.1002/mc.22781
67. Xu X, Wang J, Zhang Y, et al. Inhibition of DDX6 enhances autophagy and alleviates endoplasmic reticulum stress in Vero cells under PEDV infection. *Veterinary microbiology.* 2022;266:109350. doi:10.1016/j.vetmic.2022.109350
68. Xu W, Yu M, Qin J, et al. LACTB regulates PIK3R3 to promote autophagy and inhibit EMT and proliferation through the PI3K/AKT/mTOR signaling pathway in colorectal cancer. *Cancer Manag Res.* 2020;12:5181–5200. doi:10.2147/CMAR.S250661
69. Cutano V, Ferreira Mendes JM, Escudeiro-Lopes S, et al. LACTB exerts tumor suppressor properties in epithelial ovarian cancer through regulation of Slug. *Life Sci Alliance.* 2023;6(1):e202201510. doi:10.26508/lsa.202201510
70. Xu Y, Shi H, Wang M, et al. LACTB suppresses carcinogenesis in lung cancer and regulates the EMT pathway. *Experim Therap Med.* 2022;23(3):247. doi:10.3892/etm.2022.11172
71. Cascone A, Lalowski M, Lindholm D, et al. Unveiling the function of the mitochondrial filament-forming protein LACTB in lipid metabolism and cancer. *Cells.* 2022;11(10):1703. doi:10.3390/cells11101703
72. Ahn JW, Kim S, Na W, et al. SERBP1 affects homologous recombination-mediated DNA repair by regulation of CtIP translation during S phase. *Nucleic Acids Res.* 2015;43(13):6321–6333. doi:10.1093/nar/gkv592
73. Kostı A, de Araujo PR, Li WQ, et al. The RNA-binding protein SERBP1 functions as a novel oncogenic factor in glioblastoma by bridging cancer metabolism and epigenetic regulation. *Genome Biol.* 2020;21(1):195. doi:10.1186/s13059-020-02115-y
74. Schoft VK, Beauvais AJ, Lang C, et al. The lamina-associated polypeptide 2 (LAP2) isoforms beta, gamma and omega of zebrafish: developmental expression and behavior during the cell cycle. *J Cell Sci.* 2003;116(Pt 12):2505–2517. doi:10.1242/jcs.00450
75. Gant TM, Harris CA, Wilson KL. Roles of LAP2 proteins in nuclear assembly and DNA replication: truncated LAP2beta proteins alter lamina assembly, envelope formation, nuclear size, and DNA replication efficiency in *Xenopus laevis* extracts. *J Cell Biol.* 1999;144(6):1083–1096. doi:10.1083/jcb.144.6.1083
76. Liu C, Yu H, Shen X, et al. Prognostic significance and biological function of Lamina-associated polypeptide 2 in non-small-cell lung cancer. *OncoTargets Ther.* 2019;12:3817–3827. doi:10.2147/OTT.S179870
77. Fan X, Xie X, Yang M, et al. YBX3 mediates the metastasis of nasopharyngeal carcinoma via PI3K/AKT signaling. *Front Oncol.* 2021;11:617621. doi:10.3389/fonc.2021.617621
78. Snyder E, Soundararajan R, Sharma M, et al. Compound heterozygosity for Y box proteins causes sterility due to loss of translational repression. *PLoS Genet.* 2015;11(12):e1005690. doi:10.1371/journal.pgen.1005690
79. Zhao W, Yang H, Liu L, et al. OASL knockdown inhibits the progression of stomach adenocarcinoma by regulating the mTORC1 signaling pathway. *FASEB J.* 2023;37(3):e22824. doi:10.1096/fj.202201582R
80. Leisching G, Wiid I, Baker B. The association of OASL and Type I interferons in the pathogenesis and survival of intracellular replicating bacterial species. *Front Cell Infect Microbiol.* 2017;7:196. doi:10.3389/fcimb.2017.00196
81. Huang YZ, Zheng YX, Zhou Y, et al. OAS1, OAS2, and OAS3 contribute to epidermal keratinocyte proliferation by regulating cell cycle and augmenting IFN-1-induced Jak1-signal transducer and activator of transcription 1 phosphorylation in psoriasis. *J Invest Dermatol.* 2022;142(10):2635–2645.e9. doi:10.1016/j.jid.2022.02.018
82. Ni T, Chu Z, Tao L, et al. PTBP1 drives c-Myc-dependent gastric cancer progression and stemness. *Br J Cancer.* 2023;128(6):1005–1018. doi:10.1038/s41416-022-02118-5
83. Wang X, Li Y, Fan Y, et al. PTBP1 promotes the growth of breast cancer cells through the PTEN/Akt pathway and autophagy. *J Cell Physiol.* 2018;233(11):8930–8939. doi:10.1002/jcp.26823
84. Hollander D, Donyo M, Atias N, et al. A network-based analysis of colon cancer splicing changes reveals a tumorigenesis-favoring regulatory pathway emanating from ELK1. *Genome Res.* 2016;26(4):541–553. doi:10.1101/gr.193169.115
85. Pellegrino R, Calvisi DF, Neumann O, et al. EEF1A2 inactivates p53 by way of PI3K/AKT/mTOR-dependent stabilization of MDM4 in hepatocellular carcinoma. *Hepatology.* 2014;59(5):1886–1899. doi:10.1002/hep.26954
86. Jia L, Ge X, Du C, et al. EEF1A2 interacts with HSP90AB1 to promote lung adenocarcinoma metastasis via enhancing TGF- $\beta$ /SMAD signalling. *Br J Cancer.* 2021;124(7):1301–1311. doi:10.1038/s41416-020-01250-4
87. Xue Y, Jia X, Li L, et al. DDX5 promotes hepatocellular carcinoma tumorigenesis via Akt signaling pathway. *Biochem Biophys Res Commun.* 2018;503(4):2885–2891. doi:10.1016/j.bbrc.2018.08.063
88. Liu C, Wang L, Jiang Q, et al. Hepatoma-derived growth factor and DDX5 promote carcinogenesis and progression of endometrial cancer by activating  $\beta$ -catenin. *Front Oncol.* 2019;9:211. doi:10.3389/fonc.2019.00211
89. Li F, Ling X, Chakraborty S, et al. Role of the DEAD-box RNA helicase DDX5 (p68) in cancer DNA repair, immune suppression, cancer metabolic control, virus infection promotion, and human microbiome (microbiota) negative influence. *J Experiment Clin Cancer Res.* 2023;42(1):213. doi:10.1186/s13046-023-02787-x
90. Caravia XM, Ramirez-Martinez A, Gan P, et al. Loss of function of the nuclear envelope protein LEMD2 causes DNA damage-dependent cardiomyopathy. *J Clin Invest.* 2022;132(22):e158897. doi:10.1172/JCI158897

91. Huber MD, Guan T, Gerace L. Overlapping functions of nuclear envelope proteins NET25 (Lem2) and emerlin in regulation of extracellular signal-regulated kinase signaling in myoblast differentiation. *Mol Cell Biol.* 2009;29(21):5718–5728. doi:10.1128/MCB.00270-09
  92. Tapia O, Fong LG, Huber MD, et al. Nuclear envelope protein Lem2 is required for mouse development and regulates MAP and AKT kinases. *PLOS ONE.* 2015;10(3):e0116196. doi:10.1371/journal.pone.0116196
  93. Huang L, Zhou Y, Cao XP, et al. KPNA2 promotes migration and invasion in epithelial ovarian cancer cells by inducing epithelial-mesenchymal transition via Akt/GSK-3 $\beta$ /Snail activation. *J Cancer.* 2018;9(1):157–165. doi:10.7150/jca.20879
  94. Fan X, Li Z, Wang X, et al. Silencing of KPNA2 inhibits high glucose-induced podocyte injury via inactivation of mTORC1/p70S6K signaling pathway. *Biochem Biophys Res Commun.* 2020;521(4):1017–1023. doi:10.1016/j.bbrc.2019.10.200
  95. Chen Y, Li J, Ma J, et al. ZNF143 facilitates the growth and migration of glioma cells by regulating KPNA2-mediated Hippo signalling. *Scient Reports.* 2023;13(1):11097. doi:10.1038/s41598-023-38158-x
  96. Gao Q, Weng Z, Feng Y, et al. KPNA2 suppresses porcine epidemic diarrhea virus replication by targeting and degrading virus envelope protein through selective autophagy. *J Virol.* 2023;97(12):e0011523. doi:10.1128/jvi.00115-23
  97. Davalos V, Esteller M. Cancer epigenetics in clinical practice. *CA Cancer J Clin.* 2023;73(4):376–424. doi:10.3322/caac.21765
  98. Morel D, Jeffery D, Aspeslagh S, et al. Combining epigenetic drugs with other therapies for solid tumours - past lessons and future promise. *Nat Rev Clin Oncol.* 2020;17(2):91–107. doi:10.1038/s41571-019-0267-4
  99. Hanahan D. Hallmarks of cancer: new dimensions. *Cancer Discov.* 2022;12(1):31–46. doi:10.1158/2159-8290.CD-21-1059
  100. Mondal P, Natesh J, Penta D, et al. Progress and promises of epigenetic drugs and epigenetic diets in cancer prevention and therapy: a clinical update. *Semin Cancer Biol.* 2022;83:503–522. doi:10.1016/j.semcancer.2020.12.006
  101. Ye L, Xiang T, Fan Y, et al. The 19q13 KRAB Zinc-finger protein ZFP82 suppresses the growth and invasion of esophageal carcinoma cells through inhibiting NF- $\kappa$ B transcription and inducing apoptosis. *Epigenomics.* 2019;11(1):65–80. doi:10.2217/epi-2018-0092
  102. Le X, Mu J, Peng W, et al. DNA methylation downregulated ZDHHC1 suppresses tumor growth by altering cellular metabolism and inducing oxidative/ER stress-mediated apoptosis and pyroptosis. *Theranostics.* 2020;10(21):9495–9511. doi:10.7150/thno.45631
  103. Du Q, Zhang M, Gao A, et al. Epigenetic silencing ZSCAN23 promotes pancreatic cancer growth by activating Wnt signaling. *Cancer Biol Ther.* 2024;25(1):2302924. doi:10.1080/15384047.2024.2302924
  104. Yang W, Guo C, Herman JG, et al. Epigenetic silencing of JAM3 promotes esophageal cancer development by activating Wnt signaling. *Clin Epigenetics.* 2022;14(1):164. doi:10.1186/s13148-022-01388-3
  105. Nagaraju GP, Dariya B, Kasa P, et al. Epigenetics in hepatocellular carcinoma. *Semin Cancer Biol.* 2022;86(Pt 3):622–632. doi:10.1016/j.semcancer.2021.07.017
  106. Hernandez-Meza G, von Felden J, Gonzalez-Kozlova EE, et al. DNA Methylation Profiling of Human Hepatocarcinogenesis. *Hepatology.* 2021;74(1):183–199. doi:10.1002/hep.31659
  107. He Y, Sun MM, Zhang GG, et al. Targeting PI3K/Akt signal transduction for cancer therapy. *Signal Transduct Target Ther.* 2021;6(1):425. doi:10.1038/s41392-021-00828-5
- **Targeting PI3K for cancer therapy**
108. Glaviano A, Foo ASC, Lam HY, et al. PI3K/AKT/mTOR signaling transduction pathway and targeted therapies in cancer. *Mol Cancer.* 2023;22(1):138. doi:10.1186/s12943-023-01827-6
  109. Alemi F, Raei Sadigh A, Malakoti F, et al. Molecular mechanisms involved in DNA repair in human cancers: an overview of PI3k/Akt signaling and PIKKs crosstalk. *J Cell Physiol.* 2022;237(1):313–328. doi:10.1002/jcp.30573
  110. Huang TT, Lampert EJ, Coots C, et al. Targeting the PI3K pathway and DNA damage response as a therapeutic strategy in ovarian cancer. *Cancer Treat Rev.* 2020;86:102021. doi:10.1016/j.ctrv.2020.102021
  111. O'Neil NJ, Bailey ML, Hieter P. Synthetic lethality and cancer. *Nat Rev Genet.* 2017;18(10):613–623. doi:10.1038/nrg.2017.47